*Desalination and Water Treatment*
www.deswater.com
doi: 10.1080/19443994.2013.801323

52 (2014) 3477–3488
May

Taylor & Francis
Taylor & Francis Group

# Evaluation of equilibrium, kinetic, and thermodynamic parameters for adsorption of $Cd^{2+}$ ion and methyl red dye onto amorphous poly(azomethinethioamide) resin

T. Vidhyadevi[a], A. Murugesan[a], S.S. Kalaivani[a], M.P. Premkumar[a], V. Vinoth kumar[a], L. Ravikumar[b], S. Sivanesan[a,*]

[a]*Department of Applied Science and Technology, AC Tech, Anna University, Chennai 600 025, India*
*Tel. +91 9444960106; email: sivanesh1963@gmail.com*
[b]*Department of Chemistry, C.B.M. College, Coimbatore 641 042, India*

Received 13 December 2012; Accepted 23 April 2013

ABSTRACT

Batch adsorption studies were carried out for the removal of cadmium ion ($Cd^{2+}$ ion) and methyl red (MR) from aqueous solutions using poly(azomethinethioamide) (PATA) resin which is having pendent chlorobenzylidine ring. PATA was characterized by FT-IR spectroscopy, NMR spectroscopy, transmission electron microscope (TEM), and scanning electron microscope (SEM) techniques. Parameters like pH, initial dye and metal ion concentration, adsorbent dose, and contact time have been studied. Maximum adsorption was observed at pH 6 for $Cd^{2+}$ and at 7 for MR. Langmuir, Freundlich, Dubinin–Raduskevich (D–R), and Temkin adsorption models were applied to describe the equilibrium isotherms. The maximum monolayer adsorption capacities of $Cd^{2+}$ ion and MR dye are found to be 100 and 90.9 mg/g, respectively. The adsorption of $Cd^{2+}$ ion and MR follows second-order kinetics. The thermodynamics parameters such as $\Delta G^{\circ}$, $\Delta H^{\circ}$, and $\Delta S^{\circ}$ were also evaluated. The adsorbed $Cd^{2+}$ ion and MR were eluted by treatment with 0.2 N HCl solutions, and the adsorption efficiency of the PATA was retained even after several cycles.

*Keywords:* Thioamides; Azomethine; Isotherm; Kinetics; Thermodynamics; Desorption

## 1. Introduction

Water sources have been polluted by metals and dyes all over the world due to the effluents from many industries like electroplating, battery, textile, leather, tanning, paper industries, etc. These industries release heavy metals and dyes as major pollutants into the environment [1–3]. These heavy metal ions and dyes are dangerous pollutants, causing environmental and health problems to human being and aquatic animals. Among various heavy metal ions and dyes, we had selected to remove the cadmium ion and a cationic dye methyl red (MR) from aqueous solutions due to their following harmful effects. Cadmium is a toxic metal; it affects the aquatic life and food web even at very low concentrations. The harmful effects of cadmium include lung cancer, anemia, acute and chronic effects like renal dysfunction/nephropathy, osteomalacia, itai–itai, kidney damage, etc. [4]. MR is a cationic dye and causes cancer, skin irritation, allergy, and dermatitis to humans [5]. These metals

*Corresponding author.

and dyes accumulate in living organisms and cause serious problems to the human and ecological system [6]. Hence, it is essential to remove the metal ions and dyes from wastewater, before it is transported into the natural environment. The various treatment processes available for the removal of metals and dyes are adsorption [7], membrane separation [8], coagulation-flotation [9], advanced oxidation [10], reverse osmosis [11], etc. Among them, adsorption is the popular technique in recent years due to its efficiency in removal of the pollutants. Adsorption of metals by activated carbon prepared from naturally available sources like rice husk [12], natural dye waste [13], castor seed hull [14], etc. have been studied. Similarly, adsorbents used for the adsorption of MR include annona squmosa [15], cassava (Manihot esculenta Cranz) peel waste [16], sugarcane bagasse [17], etc. Various chelating polymeric resins are also reported for the adsorption of metal ions and dyes from aqueous solutions [18–20]. The above mentioned adsorbents are found to be less effective and have very low adsorption capacity. Hence, there is a need to find a novel adsorbent with maximum adsorption capacity. If the adsorbent can be regenerated through the desorption process, without any modification in its structure, and then the process will become more effective.

The objective of the present work is to synthesize and characterize a poly(azomethine thioamide) having pendent chlorobenzyldine ring, and use it as an adsorbent for the removal $Cd^{2+}$ ion and a cationic dye (MR). Adsorption experiments were carried out under different experimental conditions like varying the solution pH, adsorbent dose, initial adsorbate concentration, and contact time. Kinetic and isotherm parameters were used to understand the adsorption mechanism of $Cd^{2+}$ ion and MR dye onto PATA. Desorption studies were carried out for the regeneration of PATA to find out the possibility of its reuse.

## 2. Materials and methods

### 2.1. Adsorbates

$CdSO_4.8H_2O$ and MR were purchased from Sigma Aldrich Chemical, India. Stock solutions of $Cd^{2+}$ ion and MR dye were prepared by dissolving a calculated amount of $CdSO_4.8H_2O$ and MR in distilled water. The initial and final concentrations of the metal and dye solutions were analyzed by the atomic absorption spectrometer (Shimadzu, Japan) and double beam UV Spectrophotometer (Shimadzu, Japan) respectively. The UV visible spectrum of the MR solution during adsorption was determined in the wavelength range of 540 nm. The MR structure is shown in Fig. 1.

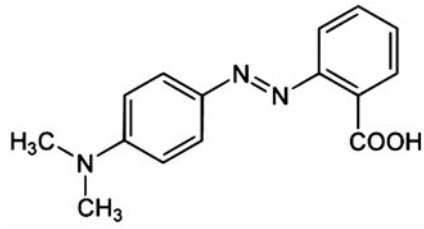


Fig. 1. Structure of MR.

### 2.2. Synthesis of adsorbent

The dicarboxylic acid monomer 2-(p-chlorobenzalimino)terephthalic acid containing an azomethine group was synthesized by condensing 0.01 mol of chlorobenzaldehyde and 0.01 mol of 2-aminoterephthalic acid in DMF (50 mL) with pyridine as a catalyst at 110°C for 4 h. The resulting dicarboxylic acid monomer was precipitated in water and recrystallized from the DMF/water solution, filtered, and dried by a vacuum pump. Polyamide was synthesized using N-methylpyrrolidine (NMP) as a solvent, and triphenylphosphite and $CaCl_2$ as the condensing agents. Dicarboxylic acid monomer and 4,4′bis(thiourea) biphenylether were taken in equimolar quantities along with triphenylphosphite, pyridine, and HCl. The reagents were stirred at a temperature of 140°C in NMP for 6 h. Then, the reaction mixture was cooled to room temperature and poured into ethanol to precipitate the polymer. The precipitated polymer was filtered, and washed with dilute $Na_2CO_3$ followed by dilute HCl to remove the unreacted monomer. It was then washed with water, ethanol, and dried in a vacuum pump. The synthesis of the PATA resin is explained in Fig. 2.

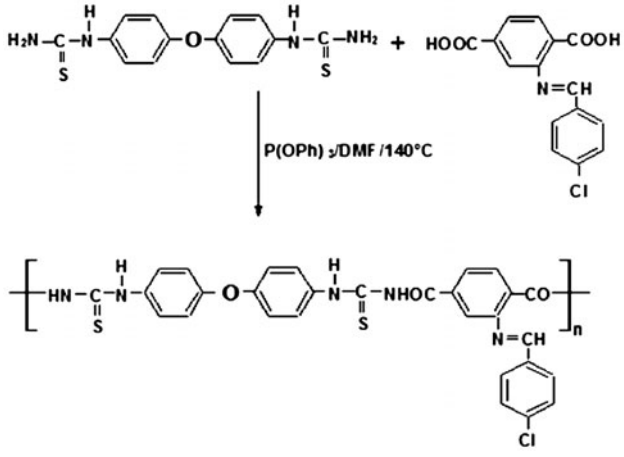


Fig. 2. Synthesis of PATA.

### 2.3. Analytical method

The FT-IR spectra of PATA resin before and after the adsorption were taken using 1725X Perkin-Elmer FT-IR spectrometer, in the spectral range of 4,000–650 $cm^{-1}$ using KBr pellet technique. The $^1H$ NMR spectrum of the PATA resin was recorded in DMSO-$d_6$ using 500 MHz FT-NMR Spectrometer. Transmission electron microscope (TEM) (Hitachi Model H-7500) was employed to determine the particle size of PATA at an acceleration voltage of 80 kV. The surface morphology of the PATA resin was studied using Leo Gemini 1530 scanning electron microscope (SEM) at an accelerating voltage of 10 kV and at a working distance of 100 μm.

### 2.4. Adsorption studies

For all adsorption experiments, 20 mL of aqueous solution of known concentrations of $Cd^{2+}$ and MR dye solutions were taken in a 250 mL conical flask containing 50 mg of PATA resin. The pH of the $Cd^{2+}$ and MR dye solutions was recorded using pH Hanna meter and solution pH was adjusted to the required value with 0.1 M NaOH or 0.1 M HCl. These flasks were agitated on a horizontal bench shaker at the constant speed of 180 rpm for 45 min to reach the equilibrium. After the mixture was centrifuged to separate the adsorbent, the solutions were analyzed by the respective spectrometer.

Batch kinetic studies were performed in 250 mL conical flasks containing 50 mg/L adsorbate solution with 50 mg of PATA. The flasks were agitated and the solutions were withdrawn from the shaker at regular time intervals and analyzed. Isotherm studies were carried out with different initial concentrations (50–250 mg/L) of $Cd^{2+}$ and MR dye solution with 50 mg of PATA. The extent of adsorption at equilibrium (mg $g^{-1}$) was calculated using the following relationship:

$$q_e = \frac{C_o - C_e}{W} \times V \quad (1)$$

where $C_o$ and $C_e$ are the initial and final adsorbate concentrations (mg/L), $V$ is the volume of the adsorbate solution (mL), and $W$ is the mass of the adsorbent (mg).

### 2.5. Desorption studies

Recycling and reuse of the spent adsorbent are essential in the adsorption process. The $Cd^{2+}$ ion and MR dye loaded PATA resin were kept in 0.2 N HCl for 24 h. It was filtered, and washed with distilled water and finally with alcohol and utilized for the adsorption cycle. Each adsorption cycle was repeated several times using the same adsorbent.

## 3. Results and discussion

### 3.1. Characterization of adsorbent

The IR spectrum of poly(azomethinethioamide) (PATA) is shown in Fig. 3. In the polymer PATA, the amide –NH, amide (I) –C=O and amide (II) –N–C=O frequencies were appeared at 3,375, 1,627, and 1,594 $cm^{-1}$, respectively. The imine –CH stretching frequency appeared at 2,277 $cm^{-1}$ (Fig. 3(a)). The –C=S stretching frequency in PATA has been found around 1,072 $cm^{-1}$. The stretching frequency of –N–C=S bands were appeared in the regions 1,400, 1,310, and 1,014 $cm^{-1}$ and it is named as –N–C=S, I, II, and III bands [21]. The above spectrum analysis supports the structure of PATA.

The $^1H$ NMR spectrum of PATA is shown in Fig. 4. The peak at $\delta = 10.8$ ppm is due to the amide

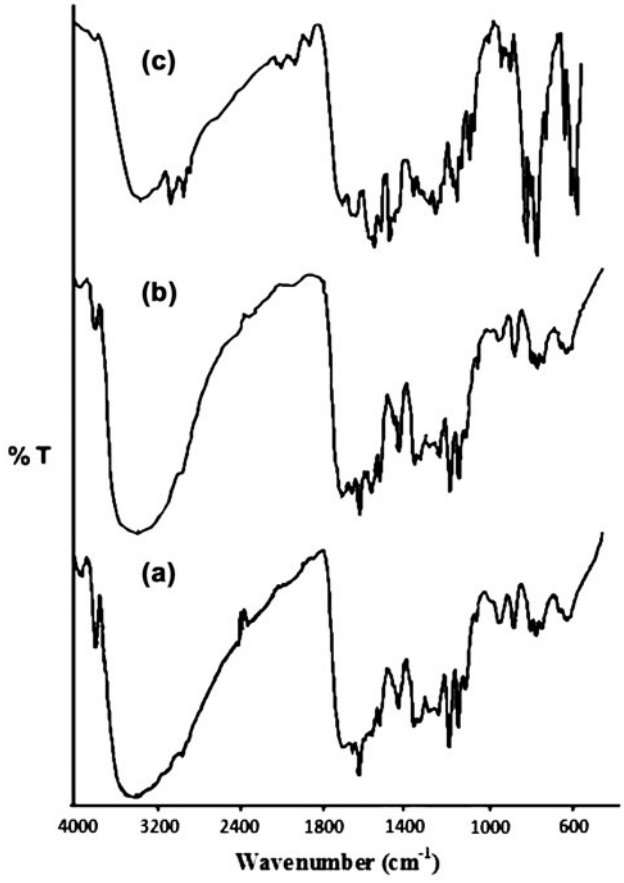


Fig. 3. FTIR spectra of (a) PATA, (b) $Cd^{2+}$ treated PATA and (c) MR treated PATA.

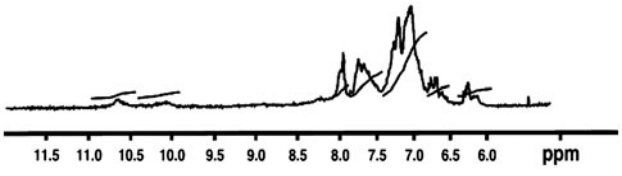


Fig. 4. $^{1}H$ NMR spectrum of PATA.

proton, and that of the –CH=N– proton appeared at $\delta = 8.2$ ppm. The complex aromatic region of the polyamide appeared as a broad signal in the region $\delta = 8.1$–$6.1$ ppm.

TEM image of PATA is shown in Fig. 5. Sample for TEM measurements was prepared by depositing a drop of colloid solution of PATA on a 400 mesh copper grid coated by an amorphous carbon film and evaporating the solvent in air at room temperature. The TEM image of PATA resin was spherical with a large size distribution ($71 \pm 58$ nm). The SEM image of the PATA clearly (Fig. 6(a)) indicates that an asymmetric surface and open pore structure is present, which may provide high internal surface area in the PATA adsorbent. The presence of pores suggests that there is a good possibility for the metal ions and dyes to be trapped and adsorbed onto the surface of the PATA. Fig. 6(b) and (c) shows that surface morphology of the treated PATA is different, before and after the adsorption of $Cd^{2+}$ ion and MR dye. The pores were completely filled after the adsorption of $Cd^{2+}$ ion and MR dye. This fact is supported by the FT-IR analysis of the $Cd^{2+}$ ion and MR dye adsorbed polymer (b) and (c) as shown in Fig. 3. When compared to plain polymers, –NH stretching frequency of amide link (3,375 $cm^{-1}$) shifted to lower frequency (3,351 and 3,362 $cm^{-1}$ for $Cd^{2+}$ and MR dye, respectively). The imine –N=CH– stretching frequency is completely disappeared in the $Cd^{2+}$ and MR dye adsorbed PATA. The carbonyl stretching frequency (1,627 $cm^{-1}$) is shifted to a higher wavelength of 1,632 and 1,645 $cm^{-1}$ for $Cd^{2+}$ and MR dye, respectively. The FT-IR spectra of $Cd^{2+}$ and MR dye treated PATA clearly suggest that the formation of metal/dye-PATA resin complexes in the solution is with the help of respective functional groups of PATA resin.

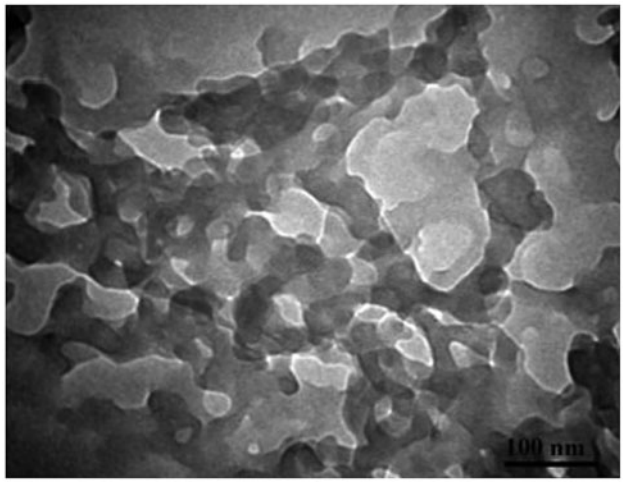


Fig. 5. TEM image of PATA.

### 3.2. Effect of pH

The pH plays an important role in the adsorption process. The percentage removal of $Cd^{2+}$ ion and MR dye was studied in the pH range of 2–8. From Fig. 7 (a), it could be seen that when the solution pH increases the percentage removal of $Cd^{2+}$ ion and MR dye also increases. The maximum percentage removal of $Cd^{2+}$ ion and MR dye occurred in pH 6 and 7, respectively. Hence an optimal pH value of 6 and 7 were fixed for further adsorption studies of $Cd^{2+}$ ion and MR dye respectively. The maximum removal at this particular pH is due to the presence of different functional groups (carbonyl, amide) on PATA, and the zero point charge ($pH_{zpc}$) of the PATA. The $pH_{zpc}$

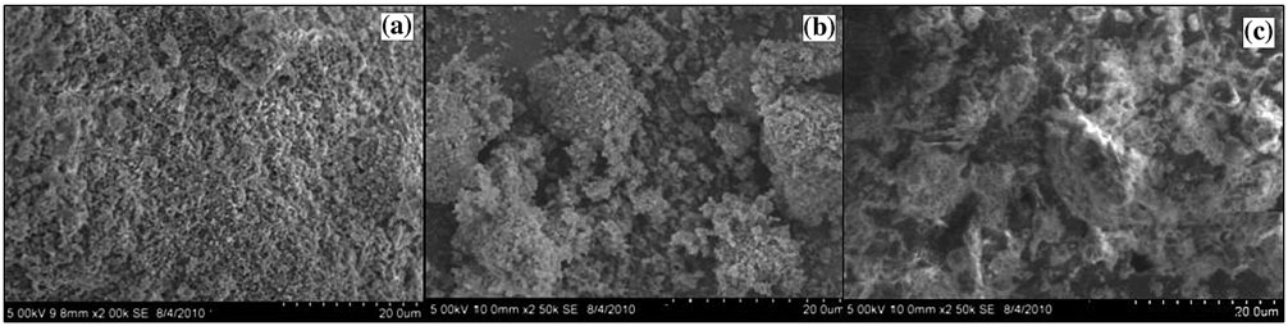


Fig. 6. (a) SEM images of PATA, (b) MR and (c) $Cd^{2+}$ treated PATA.

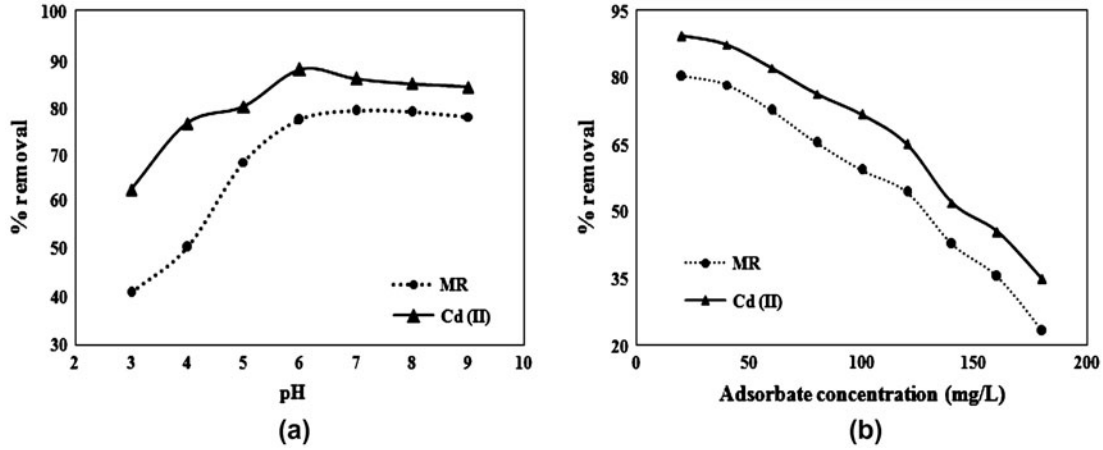


Fig. 7. Effect of (a) pH and (b) adsorbate concentration on adsorption MR and $Cd^{2+}$ ion onto PATA.

of PATA resin is found to be 4.5. The adsorption of cation is favored when the pH of the solution is greater than the zero point charge ($pH_{zpc}$) of the adsorbent. This is because, the adsorbent surface is positively charged when the solution pH is less than the $pH_{zpc}$. Since the adsorbates are cationic in nature, an increase in the solution pH above $pH_{zpc}$ increases the percentage removal of $Cd^{2+}$ ion and MR dye. Moreover, the FTIR analysis shows that PATA resin has functional groups, such as carbonyl and amide which are involved in adsorption mechanism.

### 3.3. Effect of adsorbent dose

The PATA dose is an important parameter in batch adsorption studies, as it determines the adsorption capacity of PATA, which may be attributed to the availability of more binding sites and increased surface area. The percentage removal of the $Cd^{2+}$ ion and MR dye increases with an increase in the PATA dose (figure not shown) initially and thereafter remains constant. Since, the active sites were filled up at an adsorbent dose of 40 mg; further addition of the adsorbent would not produce any considerable change in the percentage removal. So the optimum adsorbent dose of 40 mg was fixed for other adsorption studies.

### 3.4. Effect of adsorbate concentration

The effect of the initial adsorbate concentration on the removal of $Cd^{2+}$ ion and MR dye is shown in Fig. 7(b). An increase in the adsorbate concentration from 20 to 180 mg/L decreases the percentage removal of $Cd^{2+}$ ion and MR dye. But, the adsorption capacity increased with an increase in the initial adsorbate concentration (not shown). This is due to the higher adsorption rate and utilization of all the active sites of the PATA by the $Cd^{2+}$ ion and MR dye.

### 3.5. Adsorption isotherm

The adsorption isotherm plays an important role in the prediction adsorption mechanism and determination of the maximum adsorption capacity of the adsorbent. In this study, four linear isotherms, such as the Langmuir (Eq. 2) (Fig. 8(a)), Freundlich (Eq. (3)) (Fig. 8(b)), Dubinin–Raduskevich (D–R) (Eq. (4)) (Fig. 8(c)), and Temkin (Eq. (5)) (Fig. 8(d)) were tested. The Langmuir equation is applicable to a homogeneous adsorption system [22], while the Freundlich isotherm model assumes that adsorption occurs on a heterogeneous adsorption surface having unequally available sites with different energies of adsorption [23]. The Dubinin–Raduskevich is used to calculate the characteristic porosity and the apparent free energy of adsorption [24]. The Temkin isotherm model predicts the heat of adsorption and the adsorbate–adsorbent interaction on a surface [25]. The linear form of the studied isotherm is given as,

$$\frac{C_e}{q_e} = \frac{1}{K_L q_m} + \frac{C_e}{q_m} \tag{2}$$

$$\log q_e = \log k_f + \frac{1}{n}\log C_e \tag{3}$$

$$\log q_e = \log q_D + K_{DR}\varepsilon^2 \tag{4}$$

$$q_e = \beta \ln k_T + \beta \ln C_e \tag{5}$$

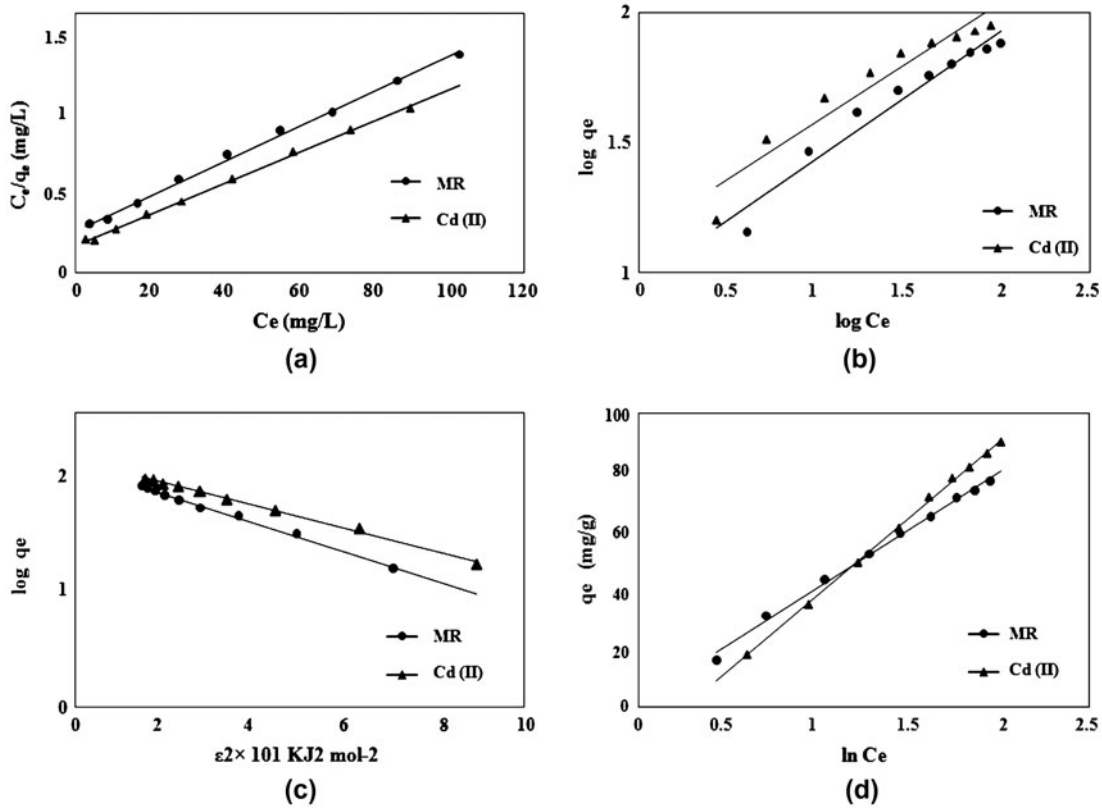


Fig. 8. Linear adsorption isotherm models (a) Langmuir, (b) Freundlich, (c) Dubinin–Raduskevich and (d) Temkin for the adsorption of MR and $Cd^{2+}$ over PATA.

where $C_e$ is the concentration of the adsorbates in solution at equilibrium (mg/L), $q_e$ is the amount of adsorbates adsorbed on unit mass of the adsorbent (mg/g), $k_L$ is the Langmuir constant related to the energy of adsorption (L/mg), and $q_m$ is the maximum amount of the adsorption with complete monolayer coverage on the adsorbent surface (mg/g). $k_f$ and $1/n$ are the Freundlich constants related to the adsorption capacity and intensity of adsorption, respectively. $K_{DR}$ is the constant related to the mean free energy of adsorption ($mol^2/kJ^2$), $\varepsilon$ is a polyanyi potential (J/mol), which is related to the equilibrium concentration $C_e$ (mg/L) and $q_D$ is the theoretical saturation capacity (mg/g). $\beta = (RT)/b$, "$b$" is the Temkin constant related to the heats of adsorption, $R$ is the universal gas constant (8.314 J/mol K), and "$T$" is the temperature in Kelvin.

Moreover, the adsorption equilibrium explained by the Langmuir equation can be expressed in terms of dimensionless constant, called the separation factor $R_L$ [26]

$$R_{\mathrm{L}} = \frac{1}{1 + K_{\mathrm{L}} C_{\mathrm{o}}} \tag{6}$$

The $R_L$ value is used to determine the favorability of the adsorption process. The adsorption is favorable ($0 < R_L < 1$) or unfavorable ($R_L > 1$) or linear ($R_L = 1$) or irreversible ($R_L = 0$). The calculated $R_L$ values are less than unity, indicating that PATA is a suitable adsorbent for the adsorption of $Cd^{2+}$ ion and MR dye. The $R_L$ values of cadmium ion (0.3679–0.0606) and MR dye (0.4849–0.0947) indicate that the adsorption process is favorable.

The estimated parameters of these models have been evaluated and the correlation coefficients of these models are given in Table 1. The experimental data yielded excellent fits in the following isotherms order for Cd (II) and MR dye: Temkin > Langmuir > Dubinin–Raduskevich > Freundlich and Langmuir = Dubinin–Raduskevich > Temkin > Freundlich respectively, based on their correlation coefficient values.

The Freundlich constant $K_F$ value of $Cd^{2+}$ (15.52) is greater than that of the MR dye (10.57) suggesting that $Cd^{2+}$ has greater adsorption tendency towards PATA than the MR dye. The values of mean free energy $\left(E = \frac{1}{\sqrt{2K_{DR}}}\right)$ are used in predicting the adsorption mechanisms; if $E < 8$ kJ/mol, the adsorption process is physical in nature, and if $E$ is between 8 and

Table 1
Isotherm parameters for the adsorption of $Cd^{2+}$and MR over PATA

| Isotherm model | Parameters | $Cd^{2+}$ ion | MR dye |
|---|---|---|---|
| Langmuir | K(L/mg) | 0.0862 | 0.05314 |
| | $q_m$ (mg/g) | 100 | 90.9 |
| | $R^2$ | 0.998 | 0.997 |
| Freudlich | $K_f$ (mg/g) | 15.52 | 10.57 |
| | $n$ | 2.3809 | 2.2124 |
| | $R^2$ | 0.922 | 0.950 |
| Dubinin–Raduskevich (D–R) | $q_d$ (mg/g) | 127.35 | 114.55 |
| | $E$ (J/mol) | 2.318 | 2.058 |
| | $R^2$ | 0.996 | 0.997 |
| Temkin | $\alpha$ (L/mg) | 0.5492 | 1.10785 |
| | $\beta$ ($mg^{-1}$) | 51.90 | 39.07 |
| | $R^2$ | 0.999 | 0.995 |

16 kJ/mol the adsorption process is due to ion exchange. In the present study, the numerical values of adsorption of the mean free energy for $Cd^{2+}$ ion and MR are found to be 2.318 and 2.058 kJ/mol, which correspond to the physical process.

The maximum monolayer adsorption capacity, calculated from the Langmuir isotherm for $Cd^{2+}$ ion and MR dye, is found to be 100 and 90.909 mg/g, respectively. The comparison of the maximum monolayer adsorption capacity of $Cd^{2+}$ ion and MR dye onto various adsorbents is represented in Table 2.

### 3.6. Adsorption kinetics

Contact time is an important factor which can reflect the adsorption kinetics of the PATA for a given initial metal and dye concentration (50 mg/L) by fixed amount of the adsorbent dose (50 mg). Fig. 9(a) shows the effect of the contact time for the removal of the $Cd^{2+}$ and MR dye onto the PATA. The adsorption rate of the $Cd^{2+}$ and MR dye increases considerably with increasing contact time up to 45 min, and thereafter, the rate of $Cd^{2+}$ and MR dye removal remains constant. The adsorption efficiency of $Cd^{2+}$ and MR dye removal was higher in the beginning due to a larger surface area of the PATA being available for the adsorption of $Cd^{2+}$ and MR dye. Later as the adsorbed $Cd^{2+}$ and MR dye forms a monolayer, the capacity of the PATA gets exhausted and then the uptake rate is controlled by the rate at which the $Cd^{2+}$ and MR dye are transported from the exterior to the interior sites of the PATA particles. This may be attributed to a steady-state approximation and quasi-equilibrium situation. Although at higher contact time, saturation stage was attained due to the accumulation of the adsorption sites by the $Cd^{2+}$ and MR dye. Therefore, the optimum contact time was selected as 45 min for all the batch experiments.

The adsorption rates of $Cd^{2+}$ ion and MR dye onto PATA were analyzed by two different kinetics models, namely pseudo-first-order and pseudo-second-order.

The pseudo-first-order kinetic model [34] can be expressed as

$$\log(q_e - q_t) = \log q_e - \frac{k_{ad}}{2.303} t \quad (7)$$

The pseudo-second-order kinetic model [35] can be expressed as

$$\frac{t}{q_t} = \frac{1}{h} + \frac{1}{q_e} t \quad (8)$$

Table 2
Comparison of maximum monolayer capacity for adsorption of $Cd^{2+}$ and MR onto various adsorbents

| Adsorbent | Adsorption capacity (mg/g) | | References |
|---|---|---|---|
| | $Cd^{2+}$ ion | MR dye | |
| Castor seed hull | 5.8 | – | [14] |
| Rice husk ash | 6.57 | – | [27] |
| Polystryrene supported chelating polymeric resin | 12.305 | – | [28] |
| Cashew nut shell | 14.29 | – | [29] |
| Jack fruit seed carbon | 0.695 | – | [30] |
| Granular activated carbon | – | 1.176 | [31] |
| Annona squmosa seed | – | 40.486 | [15] |
| Banana pseudostem fibers | | 66.68–87.64 | [32] |
| Cassava (Manihot esculenta Cranz) peel waste | | 38.60–52.90 | [16] |
| Annona squmosa seed | | 5.176–27.68 | [33] |
| PATA | 100 | 90.9 | Present study |

where $q_t$ is the amount of adsorbates adsorbed on the adsorbent at time $t$ (mg/g); $k_{ad}$ is the equilibrium rate constant of the pseudo-first-order kinetics ($min^{-1}$), $q_e$ is the equilibrium adsorption capacity and $t$ is the contact time (min); and h is the initial adsorption rate (mg/g/min), $h = kq_e^2$, where $k$ is the rate constant for pseudo-second-order kinetics (g/mg/min).

The rate constants predicted equilibrium uptakes and the corresponding correlation coefficients for the adsorbent PATA are summarized in Table 3. The $k_{ad}$ and $q_e$ values (from Eq. (7)) are calculated from the slope and intercept of the plot of log ($q_e - q_t$) vs. "t" as shown in Fig. 9(b). The parameters $q_e$, "k" and $h$ can be evaluated from the slope and intercept of the linear plot of $t/q_t$ vs. $t$ as shown in Fig. 9(c).

The experimental data deviated from linearity for the pseudo-first-order equation. The calculated $q_e$ values which differ from the experimental $q_e$ values and low correlation coefficients ($R^2$) values indicate that the adsorption of $Cd^{2+}$ ion and MR dye fitted poorly with the pseudo-first-order kinetic model. But in the case of the pseudo-second-order kinetic model, the $R^2$ values are close to unity and the calculated $q_e$ values are close to the experimental $q_e$ values. This suggests that, the adsorption system can be well represented by the pseudo-second-order model for the adsorption of $Cd^{2+}$ ion and MR dye by PATA.

### 3.7. Adsorption mechanism

The kinetic results were analyzed by intra particle diffusion model to elucidate the adsorption mechanism. The intra particle diffusion model [36] is expressed as

$$q_t = k_p t^{1/2} + C \tag{9}$$

where $k_p$ is the intra particle diffusion rate constant (mg/(g $min^{1/2}$)) and $C$ (mg/g) is a constant that gives an idea about the thickness of the boundary layer.

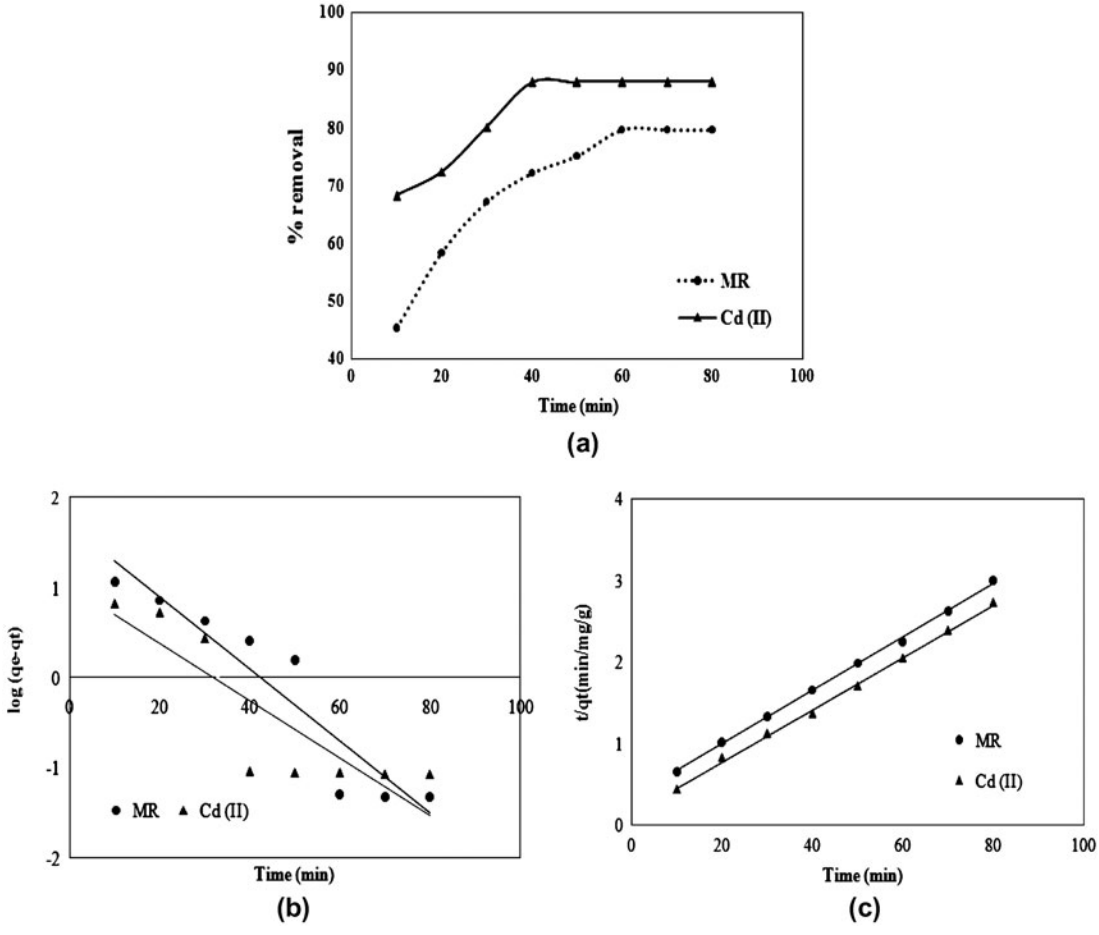


Fig. 9. (a) Effect of contact time (b) pseudo-first-order model and (c) pseudo-second-order model for adsorption of MR and $Cd^{2+}$ onto PATA.

Table 3
Kinetic models constants for adsorption of $Cd^{2+}$ and MR dye onto PATA

| Kinetic model | Parameters | $Cd^{2+}$ ion | MR dye |
|---|---|---|---|
| Pseudo-first order | $k_{ad}$ ($min^{-1}$) | 0.071 | 0.092 |
| | $q_{e,cal}$ (mg/g) | 10.423 | 50.23 |
| | $R^2$ | 0.756 | 0.887 |
| Pseudo-second order | $q_{e,cal}$ (mg/g) | 31.25 | 31.25 |
| | $k$ ($g\,mg^{-1}\,min^{-1}$) | 0.0032 | 0.0029 |
| | $h$ ($mg\,g^{-1}\,min^{-1}$) | 3.1645 | 2.8818 |
| | $q_{e,exp}$ (mg/g) | 29.4 | 26.6 |
| | $R^2$ | 0.998 | 0.998 |
| Intra particle diffusion model | $k_p$ ($mg/g\,min^{1/2}$) | 1.993 | 1.244 |
| | $C$ | 10.35 | 19.44 |
| | $R^2$ | 0.926 | 0.835 |

This model was plotted in order to verify the influence of the mass transfer resistance on the binding of $Cd^{2+}$ ion and MR dye onto the PATA (Fig. 10). Three different changes are observed in the plot (Fig. 10) of $q_t$ vs."$t^{1/2}$". In the first part, the adsorbate molecules have moved from the bulk solution to the external surface of the PATA. The second portion of the curve corresponds to the particle diffusion, where, the $Cd^{2+}$ ion and MR dye molecules have moved to the interior of the PATA. The third portion corresponds to the adsorption of the $Cd^{2+}$ ion and MR dye on the interior surface of the pores of the PATA. If the regression of the plot ($q_t$ vs. $t^{1/2}$) is linear and passes through the origin, then intra particle diffusion is the rate-determining step. However, in this study, the linear plots for $Cd^{2+}$ ion and MR dye did not pass through the origin. Such a deviation from the origin indicates that pore diffusion is the controlling step and not film diffusion. The calculated intra particle diffusion coefficient $k_p$ and $R^2$ values are listed in Table 3.

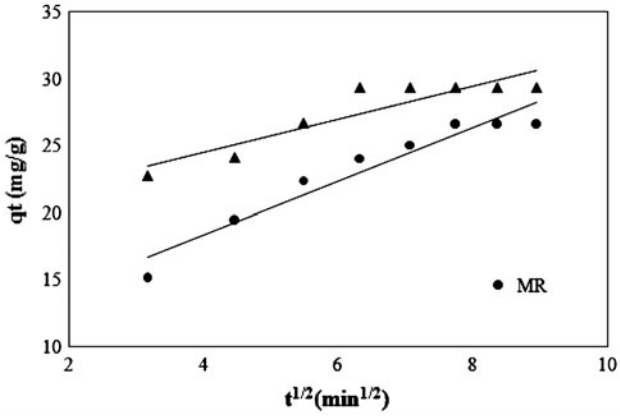


Fig. 10. Intra particle diffusion model for adsorption of MR and $Cd^{2+}$ onto PATA.

### 3.8. Effect of temperature

The adsorption of $Cd^{2+}$ ion and MR dye on PATA was investigated as a function of temperature and the maximum removal was obtained at 30°C. Experiments were performed at different temperatures of 30, 40, 50, and 60°C for the initial adsorbates concentration of 50 and 100 mg/L at constant adsorbent dose of 50 mg. The percentage removal $Cd^{2+}$ ion and MR dye decreased, as we increase the temperature from 30 to 60°C (Fig. 11). This is mainly due to the decreased surface activity, suggesting that adsorption of $Cd^{2+}$ ion and MR dye on PATA was an exothermic process.

### 3.9. Adsorption thermodynamics

Thermodynamic studies of an adsorption process are necessary in order to determine whether a process will occur spontaneously or not. Thermodynamic parameters, such as free energy ($\Delta G^\circ$), enthalpy ($\Delta H^\circ$) and entropy ($\Delta S^\circ$) change of adsorption can be evaluated from the following Eqs. (10)–(13) [37]

$$K_C = \frac{K_{ae}}{C_e} \tag{10}$$

$$\Delta G^\circ = -RT \ln K_C \tag{11}$$

$$\Delta G^\circ = \Delta H^\circ - T\Delta S^\circ \tag{12}$$

$$\log K_c = \frac{\Delta S^\circ}{2.303R} - \frac{\Delta H^\circ}{2.303RT} \tag{13}$$

where $K_c$ is the equilibrium constant, $C_e$ is the adsorbate equilibrium concentration in solution (mg/L), and $C_{ae}$ is the amount of adsorbates adsorbed on the adsorbent per liter of solution at equilibrium (mg/L). $\Delta G^\circ$, $\Delta H^\circ$, and $\Delta S^\circ$ are changes in Gibbs free energy (kJ/mol), enthalpy (kJ/mol), and entropy (J/mol/K), respectively. $R$ is the gas constant (8.314 J/mol/K), $T$ is the temperature ($K$). The values of $\Delta H^\circ$ and $\Delta S^\circ$ are determined from the slope and the intercept of the plots of log $K_c$ vs. $1/T$ (Fig. 11). The $\Delta G^\circ$ values were calculated from the thermodynamic experimental values using Eq. (11). Percentage removal of $Cd^{2+}$ ion and MR dye on PATA decreased when the temperature was increased from 303 to 333 K shown in Fig. 11. The calculated values of thermodynamic parameters are given in Table 4. The negative $\Delta G^\circ$ at different temperatures indicates the spontaneous nature of the adsorption of $Cd^{2+}$ ion and MR dye onto the PATA. The negative $\Delta H^\circ$ value suggests the exothermic nature of the process, it would be expected that the increase in temperature

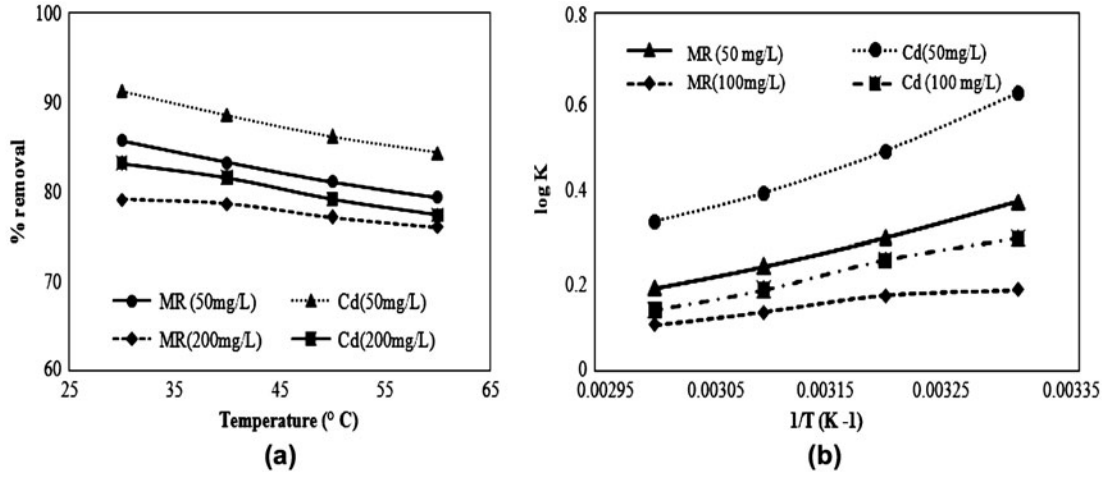


Fig. 11. (a) Effect of temperature (b) plot of log $K_c$ vs. $1/T$ for adsorption of MR and $Cd^{2+}$ onto PATA.

Table 4
Thermodynamic parameters for the adsorption of $Cd^{2+}$ and MR over PATA

| Parameters | Temperature (K) | $Cd^{2+}$ ion | | MR dye | |
|---|---|---|---|---|---|
| | | 50 m/L | 100 mg/L | 50 mg/L | 100 mg/L |
| $-\Delta H^{\circ}$ (kJ.mol$^{-1}$) | | 18.352 | 10.391 | 12.264 | 5.139 |
| $-\Delta S^{\circ}$ (kJ.mol$^{-1}$) | | 48.92 | 28.573 | 33.335 | 13.378 |
| $-\Delta G^{\circ}$(kJ.mol$^{-1}$) | 303 | 0.950 | 1.559 | 0.456 | 0.742 |
| | 313 | 0.775 | 1.272 | 0.437 | 0.642 |
| | 323 | 0.626 | 1.061 | 0.349 | 0.486 |
| | 333 | 0.515 | 0.921 | 0.286 | 0.375 |

would result in an increase in adsorption capacity [38] and the negative $\Delta S^{\circ}$ can describe the randomness at the PATA-solution interface during the adsorption of $Cd^{2+}$ ion and MR dye onto the PATA.

### 3.10. Desorption studies

Desorption studies help to elucidate the nature of the adsorption and recycling of the spent adsorbent.

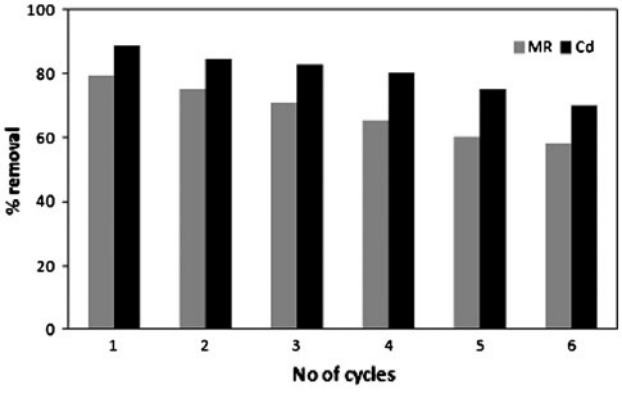


Fig. 12. Recyclability of PATA.

After the adsorption experiment, the $Cd^{2+}$ ion and MR dye loaded PATA were separated by centrifugation and the filtrates were discarded. Since $Cd^{2+}$ ion and MR are cationic in nature, it can be easily precipitated as chloride salts using hydrochloric acid. The adsorbates loaded PATA was washed with water several times to remove the unadsorbed $Cd^{2+}$ ion and MR dye. After that, the PATA was kept in a 0.2 N HCl solution for about 6 h, then washed with deionized water to remove any residual desorbing solution, and utilized for the adsorption cycle. The regenerated PATA was used again for four adsorption cycles, and the results are given in Fig. 12. Regeneration studies show that adsorption using the PATA is a physical process.

## 4. Conclusion

PATA is a promising adsorbent for the removal of $Cd^{2+}$ ion and MR dye from an aqueous solution. The maximum adsorption of $Cd^{2+}$ ion and MR dye by PATA occurred at pH 6 and 7, respectively. The removal efficiency increased with decrease in the adsorbate concentration and increase in the dose of

the adsorbent. The experimental data yielded shows excellent fit with the following isotherms in the order for $Cd^{2+}$ ion and for MR dye: Temkin > Langmuir > Dubinin–Raduskevich > Freundlich and Langmuir = Dubinin–Raduskevich > Temkin > Freundlich, respectively. The adsorption mechanism determined from the intra particle diffusion model suggests that the adsorption process occurs by the pore diffusion mechanism. The PATA adsorbent has been regenerated and reused for at least six cycles for the $Cd^{2+}$ ion and MR dye removal with a little decrease in the percentage removal. The overall results reveal that the chelating resin PATA can be used in the treatment of wastewater containing $Cd^{2+}$ and MR.

## References


[1] P. Senthil Kumar, S. Ramalingam, C. Senthamarai, M. Niranjanaa, P. Vijayalakshmi, S. Sivanesan, Adsorption of dye from aqueous solution by cashew nut shell: Studies on equilibrium isotherm, kinetics and thermodynamics of interactions, Desalination 261 (2010) 52–60.

[2] P. SenthilKumar, S. Ramalingam, V. Sathyaselvabala, S. Dinesh Kirupha, S. Sivanesan, Removal of copper(II) ions from aqueous solution by adsorption using cashew nut shell, Desalination 266 (2011) 63–71.

[3] P. Rajkumar, P. Senthil Kumar, S. Dinesh Kirupha, T. Vidhyadevi, J. Nandagopal, S. Sivanesan, Adsorption of Pb (II) Ions onto surface modified guazuma ulmifolia seeds and batch adsorber design, Environ. Prog. Sustain Energy (2012) doi:10.1002/ep.11632.

[4] H.A. Jamali, A.H. Mahvi, S. Nazmara, Removal of cadmium from aqueous solutions by hazel nut shell, World Appl. Sci. J. 5 (2009) 16–20.

[5] M.A. Mahmoud, A. Poncheri, Y. Badr, M.G.A. Wahed, Photocatalytic degradation of methyl red dye, South Afr. J. Sci. 105 (2009) 299.

[6] X. Zhao, Q. Li, X. Zhang, H. Su, K. Lan, A. Chen, Simultaneous removal of metal ions and methyl orange by combined selective adsorption and photocatalysis, Environ. Prog. Sustain Energy 30 (2011) 567–575.

[7] Ya Pang, Guangming Zeng, Lin Tang, Yi Zhang, Yuanyuan Liu, Xiaoxia Lei, Zhen Li, Jiachao Zhang, Gengxin Xie, PEI-grafted magnetic porous powder for highly effective adsorption of heavy metal ions, Desalination 281 (2011) 278–284.

[8] A.L. Ahmad, W.A. Harris, Syafiie, B.S. Ooi, Removal of dye from wastewater of textile industry using membrane technology, J. Teknol. 36 (2002) 31–44.

[9] M. Chaf, B. Gourich, A.H. Essadki, C. Vial, A. Fabregat, Comparison of electrocoagulation using iron and aluminium electrodes with chemical coagulation for the removal of a highly soluble acid dye, Desalination 281 (2011) 285–292.

[10] A.S. Stasinakis, Use of selected advanced oxidation processes (AOPS) for wastewater treatment—a mini review, Global Nest J. 10(3) (2008) 376–385.

[11] E. Kurt, E. Kurt, D.Y. Koseoglu-Imer, N. Dizge, S. Chellam, I. Koyuncu, Pilot-scale evaluation of nanofiltration and reverse osmosis for process reuse of segregated textile dyewash wastewater, Desalination 302 (2012) 24–32.

[12] R. Chand, T. Watari, K. Inoue, H. Kawakita, H.N. Luitel, D. Parajuli, T. Torikai, M. Yada, Selective adsorption of precious metals from hydrochloric acid solutions using porous carbon prepared from barley straw and rice husk, Miner Eng. 22 (2009) 1277–1282.

[13] S.P. Vankar, R. Sarswat, D.S. Malik, Biosorption of lead and cadmium ions from aqueous solutions onto natural dye waste of hibiscus rosa sinensis, Environ. Prog. Sustain Energy 29 (2010) 421–427.

[14] T.K. Sen, M. Mohammod, S. Maitra, B.K. Dutta, Removal of cadmium from aqueous solution using castor seed hull: a kinetic and equilibrium study, clean—soil, Air, Water 38(9) (2010) 850–858.

[15] T. Santhi, S. Manonmani, T. Smitha, Removal of methyl red from aqueous solution by activated carbon prepared from the annona squmosa seed by adsorption, Chem. Eng. Res. Bull. 14 (2010) 11–28.

[16] P. Adowei, M. Horsfall, A.I. Spiff, Adsorption of methyl red from aqueous solution by activated carbon produced from cassava (manihot esculenta cranz) peel waste, Innov. Sci. Eng. 2 (2012) 24.

[17] A.G.L. Abdullah, M.A. Mohd Salleh, M.K.S. Mazlina, M.J. Megat Mohd Noor, M.R. Osman, R. Wagiran, S. Sobri, Azo dye removal by adsorption using waste biomass:Sugarcane bagasse, Int. J. Eng. Technol. 2 (2005) 8–13.

[18] Rajangam Vinodh, Rajangam Padmavathi, Dharmalingam Sangeetha, Separation of heavy metals from water samples using anion exchange polymers by adsorption process, Desalination 267 (2011) 267–276.

[19] F.L. Fu, Q.R. Xuan, R.M. Chen, Y. Xiong, Removal of Cu2+ and dye from wastewater using the heavy metal precipitant N,N-bis-(dithiocarboxy) piperazine, Environ. Chem. Lett. 4 (2006) 41–44.

[20] S.R. Sandeman, V.M. Gun'ko, O.M. Bakalinska, C.A. Howell, Y. Zheng, M.T. Kartel, G.J. Phillips, S.V. Mikhalovsky, Adsorption of anionic and cationic dyes by activated carbons, PVA hydrogels, and PVA/AC composite, J. Colloid Interf. Sci. 358 (2011) 582–592.

[21] C.N.R. Rao, R. Venkataraghavan, The C=S stretching frequency and the "–N–C=S bands" in the infrared, Spectrochim. Acta 18(4) (1962) 541–547.

[22] I. Langmuir, The adsorption of gases on plane surface of glass, mica and platinum, J. Am. Chem. Soc. 40 (1918) 1361–1403.

[23] H.M.F. Freundlich, Over the adsorption in solution, J. Phys. Chem. 57 (1906) 384–470.

[24] M.M. Dubinin, L.V. Radushkevich, Equation of the characteristic curve of activated charcoal, Chem Zent. 1 (1947) 875.

[25] M.J. Temkin, V. Pyzhev, Recent modifications to Langmuir isothersms, Acta Physiochim. USSR 12 (1940) 217–225.

[26] K.R. Hall, L.C. Eagleton, A. Acrivos, T. Vermeulen, Pore and solid-diffusion kinetics in fixed-bed adsorption under constant-pattern conditions, Ind. Eng. Chem. Fund. 5(2) (1966) 212–223.

[27] A.G. El-Said, N.A. Badawy, S.E. Garamon, Adsorption of cadmium (II) and mercury (II) onto natural adsorbent rice husk ash (RHA) from aqueous solutions: Study in single and binary system, Am. J. Sci. 6(12) (2010) 400–409.

[28] A. Ravikumar Reddy, K. Hussain Reddy, Heavy metal ion uptake properties of polystyrene-supported chelating polymer resins, Proc. Indian Acad. Sci. (Chem. Sci.). 115 (3) (2003) 155–160.

[29] S. Tangjuank, N. Insuk, J. Tontrakoon, V. Udeye, Adsorption of lead(II) and cadmium (II) ions from aqueous solutions by adsorption on activated carbon prepared from cashew nut shells, World Acad. Sci. Eng Technol. 52 (2009) 110–116.

[30] N. Kannan, T. Veemaraj, Batch adsorption dynamics and equilibrium studies for the removal of cadmium (II) ions from aqueous solution Using jack fruit seed and commercial activated carbons—a comparative study, Elec. J. Environ. Agri. Food Chem. 9(2) (2010) 327–336.

[31] A.U. Itodo, A. Usman, G. Akinrinmade, H.U. Itodo, V.C. Ugboaja, Performance assessment of received and formulated carbon animals: A comparative adsorption isotherm test, J. Environ. Prot. 3 (2012) 288–295.

[32] H.M. Rosemal, M. Haris, K. Sathasivam, The removal of methyl red from aqueous solutions using banana pseudostem fibers, Am. J. Appl. Sci. 6(9) (2009) 1690–1700.
[33] T. Santhi, S. Manonmani, T. Smithaa, Kinetics and isotherm studies on cationic dyes adsorption onto annona squmosa seed activated carbon, Int. J. Eng. Sci. Technol. 2(3) (2010) 287–295.
[34] S. Lagergren, About the theory of so-called adsorption of soluble substances, Kungliga Sven. Vetensk Handl. 24 (1898) 1–39.
[35] Y.S. Ho, G. McKay, Pseudo-second order model for sorption processes, Process Biochem. 34 (1999) 451–465.
[36] W.J. Weber, Jr., J.C. Morriss, Kinetics of adsorption on carbon from solution, J. Sanit. Eng. Div. Proc. Am. S Civ. Eng. 89 (1963) 31–60.
[37] V.V. Konovalova, G.M. Dmytrenko, R.R. Nigmatullin, M.T. Bryk, P.I. Gvozdyak, Chromium (VI) reduction in a membrane bioreactor with immobilized pseudomonas cells, Enz. Microb. Technol. 33 (2003) 899–907.
[38] Y. Nuhoglu, E. Malkoc, Thermodynamic and kinetics studies for environmentally friendly Ni(II) biosorption using waste pomace of olive factory, Bioresour. Technol. 100 (2009) 2375–2380.